Early layer formation on K-feldspar during fluidized bed combustion with phosphorus-rich fuel

(article starts on next page)

Full Length Article

Early layer formation on K-feldspar during fluidized bed combustion with phosphorus-rich fuel

Robin Faust [a,*], Katharina Fürsatz [b,c,d], Panida Aonsamang [a], Marcus Sandberg [a], Matthias Kuba [b,c], Nils Skoglund [d], Pavleta Knutsson [a]
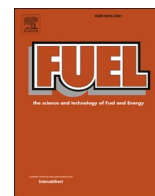
[a] Department of Chemistry and Chemical Engineering, Chalmers University of Technology, Kemigården 4, 412 96 Gothenburg, Sweden
[b] BEST – Bioenergy and Sustainable Technologies GmbH, Inffeldgasse 21b, 8010 Graz, Austria
[c] TU Wien, Institute of Chemical, Environmental and Bioscience Engineering (ICEBE), Getreidemarkt 9/166, 1060 Vienna, Austria
[d] Thermochemical Energy Conversion Laboratory, Department of Applied Physics and Electronics, Umeå University, SE-901 87 Umeå, Sweden

ABSTRACT

K-feldspar was utilized as bed material for fluidized bed combustion of bark, chicken manure, and their mixture. Bed samples were extracted after 4 and 8 h and the samples were analyzed with scanning electron microscopy to study the impact of P-rich chicken manure on the bed material. The results were compared to fixed bed exposures with different orthophosphates to investigate their influence in detail.

The fresh bed material used for this study exhibited an uneven surface with many cavities which facilitated the deposition and retention of the fuel ash. Utilizing pure chicken manure as fuel led to the formation of Ca- and P-rich particles which accumulated in these cavities. At the same time, larger ash particles were formed which consisted of the elements found in chicken manure ash. The co-combustion of bark and chicken manure led to the interaction of the two ash fractions and the formation of a thicker ash layer, which consisted of elements from both fuel ashes, namely Ca, P, Si, K and S. The layer appeared to be partially molten which could be favorable for the deposition of ash particles and thereby the formation of a mixed Ca/K-phosphate. Fixed bed exposures of the K-feldspar particles with Na_3PO_4 or K_3PO_4 caused particle agglomeration which means presence of alkali-phosphates should be limited.

The co-combustion of bark with chicken manure showed promising results both regarding a shift from Ca-phosphates to more bioavailable Ca/K-phosphates and an acceleration in ash layer formation. The formation of an ash layer after only 4 h of exposure with the mixture of bark and chicken manure could be advantageous for catalytic activation of the bed material.

1. Introduction

The change in global energy supply to meet the targets outlined by IPCC for maximum 1.5°global warming by 2050 [1]. requires not only an increased use of bioenergy to replace fossil fuel dependency, but also a broader view on the sustainability of fuel feedstock. Important aspects linked to this are the planetary boundaries [2] and sustainable development goals [3] where land use, water quality, and specifically phosphorus management are aspects intimately connected with biomass production and bioenergy.

The global phosphorus application as fertilizers (14.2 Tg/year) is more than twice as high as the regional level planetary boundary (6.2 Tg/year) (2). Phosphorus enrichment in fresh water due to runoff from fields is an environmental concern as accumulation of nutrients in water

basins can cause eutrophication which can be devastating for water organisms [4–5]. At the same time, phosphorus was declared by the European Union as a critical raw material with 100 % import reliance and 0 % end-of-life recycling [6]. Thus, there is an increased need to recirculate the bioavailable phosphorus in a controlled way.

Residual streams from biomass and food production have the possibility to play a key role in the implementation of bioenergy [7]. Some residual feedstocks could at the same time enable recycling of critical resources, like phosphorus, back into biomass production. One of these interesting residual streams is manure, which is a by-product from agriculture and farming and contains high amounts of nitrogen and phosphorus [8]. The combustion of such a phosphorus-rich feedstock can function as a pathway to concentrate the phosphorus present in the manure within the formed ash and even to contribute to an increase in

---

the bioavailability of phosphorus [9–13]. The ash accumulated during combustion could therefore be used for subsequent nutrient recovery which means that the combustion process can be seen as a sustainable process for handling manures without the loss of the valuable nutrient content. Ash from chicken manure combustion contained small amounts of toxic elements, however, the concentration was found to be within the limits for agricultural fertilizers [10]. According to Williams et al. [12] electricity production and subsequent use of fuel ash as fertilizer from turkey manure has had a positive effect on the environmental impact of manure utilization compared to the direct use on fields.

Among the existing processes for thermal conversion of biobased fuels, fluidized bed combustion is a suitable method [14]. In a fluidized bed, a bed material, usually consisting of mineral particles of around 200 – 250 μm diameter, is fluidized by a gas stream which enhances the heat distribution in the reactor. Conventionally, quartz sand is applied as bed material. Recent research attention has focused on alkali-feldspar [(K, Na)AlSi$_3$O$_8$] for fluidized bed applications with biomass, to limit the problems associated with agglomeration of quartz [9,15–21]. Additional to its agglomeration resistance, another advantage of feldspar is its inherent activity towards reducing the concentration of high molecular hydrocarbon species (i.e., tar). Tar represents an unwanted side-product occurring during the related fluidized bed gasification process [16–19]. Interactions of fuel ash and bed material lead to the formation of ash layers around the bed material particles. These layers have been assigned different properties depending on their composition – from increasing the agglomeration potential of the material [22–23] to enhancing its activity towards tar reforming and gasification reactions [17–18,24]. Bed material particle layer formation was compared in a review by Kuba et al. [25] for the most commonly employed bed materials, quartz, olivine, and feldspar. Outer layers formed on all materials by the accumulation of ash elements (i.e., inorganic elements originating from the fuel). Interactions between ash and bed material led to the formation of inner layers. Compared to olivine and quartz, the driving force for inner layer formation is weaker for feldspar, which is why differentiating between inner and outer layer was less clear [25]. A comparison between Na- and K-feldspar showed crack formation in Na-feldspar, which is why K-feldspar was deemed more suitable for fluidized bed applications [20–21,25].

Layer formation on K-feldspar exposed to phosphorus-rich chicken manure was studied by Wagner et al. [15,26]. The difference to previous studies investigating layer formation on feldspar which was exposed to woody biomass [20–21,27], was the stronger tendency to form an outer ash deposition layer instead of an inner interaction layer. However, the authors found that utilizing a mixture of bark and chicken manure as fuel, amplified layer formation. This enabled a continuation of the experiment for the scheduled 40 h, whereas the experiment utilizing pure chicken manure had to be interrupted after 11 h, due to accumulation of ash in the reactor. Layer formation analysis were in both cases conducted with samples at the end of the experiment (i.e., 11 h for pure chicken manure and 40 h for the mixture of chicken manure with bark). The difference in exposure time limits the comparability regarding layer formation. The same samples were utilized for the analysis of the fate of phosphorus performed by Häggström et al. [9] However, investigations on the catalytic activity of the same material conducted by Fürsatz et al. [18] could show that the strongest increase in surface area and H$_2$ yield occurred within the first 8 h of the experiment.

The aim of the present work is therefore to investigate the onset of layer formation mechanism on K-feldspar in fluidized beds. At early stages of the experiment, ash layers are thin and therefore challenging to investigate. The sample preparation method for electron microscopy analysis of particle cross-sections which is commonly conducted in studies on layer formation is embedding particles into epoxy and subsequently grinding with SiC paper. The surface quality achieved by this technique is insufficient to study the thin layers formed after short exposure times. In the present study, a more sophisticated sample preparation method is employed which achieves a higher surface

quality. Understanding if and how manures may present a challenge in thermal conversion will aid in their implementation in the fuel feedstock required for sustainable bioenergy. Furthermore, the specific morphologies and local conditions in the bed particles that lead to preferential accumulation of phosphorus are investigated. This knowledge can aid to facilitate a controlled layer build-up when accumulation of phosphorus together with layer activity is desired. Lastly, insight into the fate of ash-derived phosphorus could be beneficial for utilization of the ash for phosphorus recycling.

2. Experimental set-up

2.1. Bed material

K-feldspar (87 % K-feldspar, 7 % Na-feldspar, 4 % quartz, 2 % clay substance) was used as bed material in the experiments. The material was provided by Amberger Kaolinwerke (Feldspar FS 900 S), and the reported bulk density was 1100 kg/m^3. Prior to the experiments, the received particles were sieved and the range of 200 – 250 μm was selected. Finally, 550 g of the particles were filled into the reactor for each experiment.

2.2. Fuel

For the reported experiments, two biogenic fuels and a fuel mixture of those fuels were selected. Bark was chosen as a woody fuel as it is richer in ash compared to stem wood. Chicken manure is an especially ash-rich residue and contains considerable amounts of phosphorus, which is known to influence ash layer formation [28]. A fuel mixture of bark and chicken manure (0.7 kg/kg bark and 0.3 kg/kg chicken manure) was selected to further study the effect of phosphorus and its preferential accumulation during the formation of the ash layer. The main characteristics of the fuels are summarized in Table 1.

2.3. 5 kW bubbling fluidized bed combustion experiments

The combustion experiments were performed (Table 2.) in a 5 kW bubbling fluidized bed reactor, depicted in Fig. 1. Each experiment was performed with 540 g of virgin bed material and a primary airflow of 50 NL/min and a secondary airflow of 30 NL/min to ensure full combustion. The reactor was heated up electrically at a heating rate of 3 °C/min before starting the fuel feed at around 500 °C. The fuel feeding rate was around 0.7 kg/h and the aimed at operation temperature was between 800 and 830 °C. A more detailed description of the fluidized bed can be found in the work by Öhman and Nordin [29]. For this study, bed material samples were taken after 4 and 8 h. Samples taken at later periods focusing on long-term layer formation as well as ash speciation were reported previously [9,15,18] and will therefore not be part of this study.

Table 1

Main characteristics of the fuels and fuel mixtures, bark, chicken manure and the mixtures thereof which were used for this experimental campaign. [15].

	Ash content	Lower heating value	Deformation temperature
Unit	% dry basis	kJ kg^{-1}	°C
Norm	EN ISO 18122:2015–11	EN ISO 18125:2017–05	CEN/TS 15370–1:2006–12
Bark	8.1	18,180	1160
Chicken manure	25.4	13,900	>1490
70 % bark, 30 % chicken manure	13.5	16,430	>1490

Table 2
Ash composition of chicken manure, bark, and the mixture of 70 wt% bark and 30 wt% chicken manure. The values are presented in atomic % on an O-free basis. The data was obtained with XRF analysis, and the relative error of the given results is ± 2 %.

	Chicken Manure	Bark	70B 30CM
K	8.5	3.7	6.1
Na	7.4	7.4	5.5
Ca	26.4	20.5	27.5
Mg	14.1	10.0	11.4
Fe	0.7	4.3	2.1
Al	2.2	12.4	6.7
Si	5.7	36.3	20.0
P	25.7	2.4	14.5
S	2.8	1.4	2.9
Cl	6.4	1.6	3.2

2.4. Fixed bed salt exposure experiments

To study the impact of different alkali and alkaline-earth phosphates in a controlled environment, fixed bed exposures were conducted, where K-feldspar particles were mixed with different salts in an alumina crucible. The amounts of salt added were selected to resemble the bed material-ash interactions as a result of ash accumulation. To gain comparability of the exposures, the same amount of alkali and alkaline earth metals (AAEM) on a molar basis was selected. 2 g of K-feldspar was exposed at 830 °C in ambient air conditions with different types of salt added according to Table 3.

2.5. Materials analysis

Scanning electron microscopy (SEM) was performed on both particles and cross-sections of the particles using a Phenom ProX SEM. For lower magnifications, cross-sections were prepared by embedding the samples into epoxy and subsequent grinding and polishing with SiC paper. Energy-dispersive X-ray spectroscopy (EDS) point analysis was conducted on several particles and the formed ash layers to obtain information about the elemental composition. For more in-depth analysis of the samples, cross-sections of the particles were created using broad ion beam (BIB) milling with a Leica EM TIC 3X. This method provides an

Table 3
Type and amount of alkali and alkaline-earth salts (AAEM) added to 2 g of K-feldspar during the controlled fixed bed materials exposures performed to mimic the bed material-ash interactions. The selection was made on availability of orthophosphates.

AAEM	Salt	Mass
0.01 mol K^+	K_3PO_4	0.73 g
0.01 mol Na^+	$Na_3PO_4 \cdot 12H_2O$	1.31 g
0.01 mol Ca^{2+}	$CaHPO_4$	0.47 g
0.01 mol Mg^{2+}	$Mg_3(PO_4)_2 \cdot 5H_2O$	1.22 g
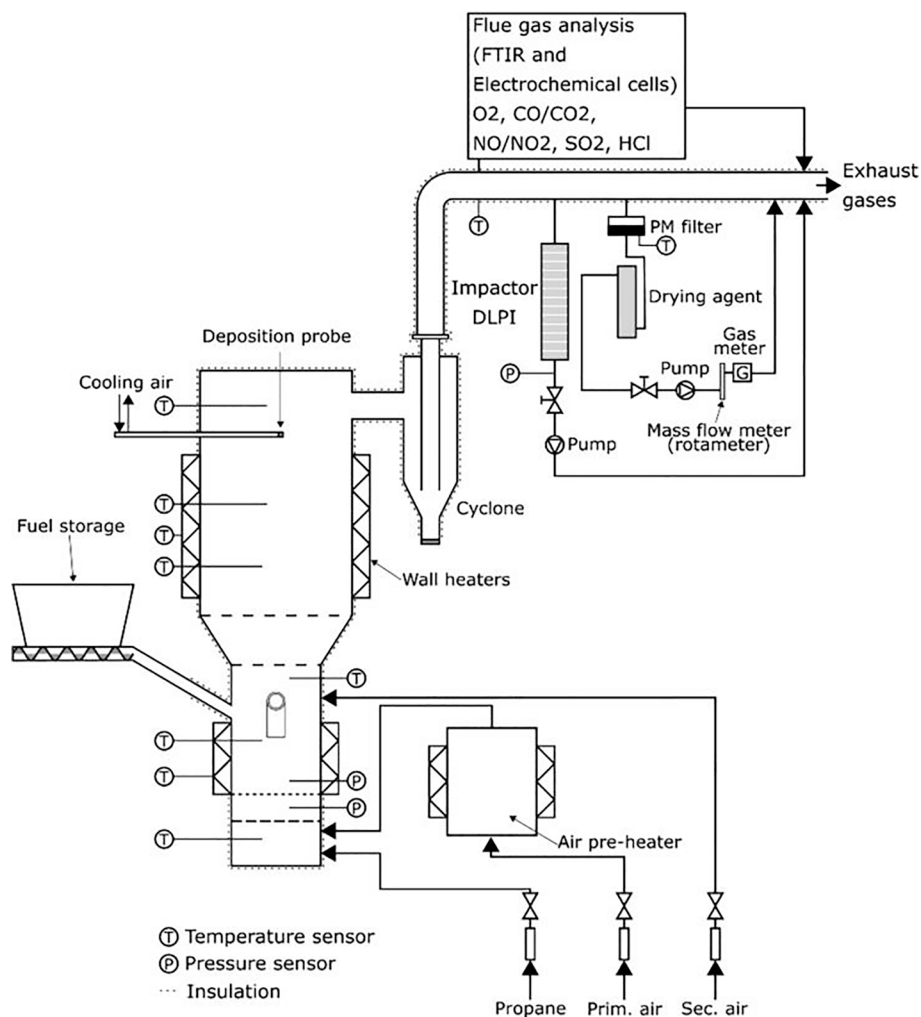
Fig. 1. Schematic representation of the 5 kW bubbling fluidized bed used for the combustion experiments with indicated temperature and pressure measurement points. [9].

improved surface quality which enables higher-resolution SEM analysis on around five typical particles. The particles are fixated between two silicon wafers with glue and polished with SiC paper prior to the BIB milling, as described previously [30–31]. The analysis of these samples was conducted with a FEI ESEM Quanta 200. To gain information on the composition of the formed ash layer, EDS line-scans were recorded which was done by recording several EDS points which were located in a line. Both electron microscopes were operated at 15 kV acceleration voltage and the back-scattered electron (BSE) signal was used for imaging.

The thickness of the layers formed around the bed particles was investigated by using ImageJ [32]. The area of the layer was measured depending on the back-scattered electron contrast, as shown in Fig. 2. Assuming spherical particles and constant layer thickness, the radius of the particle without the ash layer (r_p) was calculated by equation (1), where A_T is the total area of the particle and A_L the area of the layer. The layer thickness (d_L) could then be calculated using equation (2). This analysis requires a sufficiently thick layer which is why it was only conducted for the samples exposed for 8 h to pure chicken manure and the mixture of chicken manure and bark.

$$r_p = \sqrt{\frac{A_T - A_L}{\pi}} \tag{1}$$

$$d_L = \sqrt{\frac{A_L}{\pi} + r_p^2} - r_p \tag{2}$$

To obtain information about the amount of water leachable anions from the particles, 1 g of sample was immersed in 10 ml milli-Q water (L/S ratio 10) and stirred for 72 h. The solution obtained after leaching was analyzed by ion chromatography (Dionex ICS90) with an IonPac AS4A-SC IC column.

2.6. Fact Sage calculations

Thermodynamic equilibrium calculations were conducted with FactSage 7.2 [33]. The Equilib module was utilized to investigate the phases which are in chemical equilibrium at the conditions present in the system. Compositional data obtained from the EDS line-scans was used as input values and the elements were assumed to be present as oxides. To mimic the conditions, present during the combustion, the temperature was set to 830 °C and the pressure to 1 atm.

3. Results & discussion

3.1. Particle overview

SEM top-views and cross-sections of fresh K-feldspar particles were recorded to investigate the morphology of the particles prior to exposure

to biomass. Fig. 3 (a) and (b) show the SEM micrographs of the particles' surface and cross-sections of the K-feldspar used as a bed material in the experiments with chicken manure initially performed by Wagner et al. [15]. For comparison, SEM micrographs of the particles' surface and cross-sections of the alkali-feldspar used previously in similar studies in the dual fluidized bed gasifier at Chalmers University [16–17,20–21] are shown in Fig. 3 (c) and (d). As it can be seen from the micrographs, the K-feldspar from the current study exhibits a ragged structure [see Fig. 3 (a)] with many cavities and a higher porosity compared to the alkali-feldspar used in a previous study [20–21]. A possible reason for the observed diverse morphology could come from the difference in geological origin of the two feldspar minerals. The particles depicted in (a) and (b) are obtained from a sedimentary deposit of kaolin and have undergone weathering [34]. Compared to that, the alkali-feldspar utilized at Chalmers is mined from pegmatite rock from which the alkali-feldspar fraction is extracted [16]. The difference in morphology is reflected by the difference in reported bulk density which is 1100 kg/m³ in the present study, compared to 1400 kg/m³ for the material used in the Chalmers gasifier [16], which confirms the higher porosity of the material in the present study.

Bed material particles were collected after 4 and 8 h of operation with bark, chicken manure and a mix thereof. The morphology of the particles extracted after 8 h can be followed on the micrographs obtained using SEM, shown in Fig. 4. Already after this short exposure time, a change in particle morphology can be observed, as the previously described ragged structure of the bed material is no longer visible. This effect seems to be independent of utilized fuel and is most probably a result of a combined effect of attrition and ash layer formation. The exposure of the bed material to chicken manure [see Fig. 4 (d)], led to the formation of around 20 % particles which are not original feldspar bed material. This can be distinguished by their morphology as well as their deviating back-scattered electron contrast. As their back-scattered electron contrast is different from the original feldspar particles, one could conclude that they originate from the fuel ash. They appear homogeneous in content, however, on their surface, areas containing multiple small particles can be seen. The addition of bark to chicken manure led to the formation of rounded structures at edges of the particles (e). The cross-sections of these particles reveal the absence of pure ash particles (f). This indicates that the addition of bark ash to chicken manure ash does not lead to the agglomeration of smaller ash particles to larger structures. Rather, the addition of bark results in a possible amplification of the interaction between the two ash fractions. These findings are in agreement with what has been observed previously, where the thickest ash layer was formed, in the case when bark and chicken manure were applied together [15].
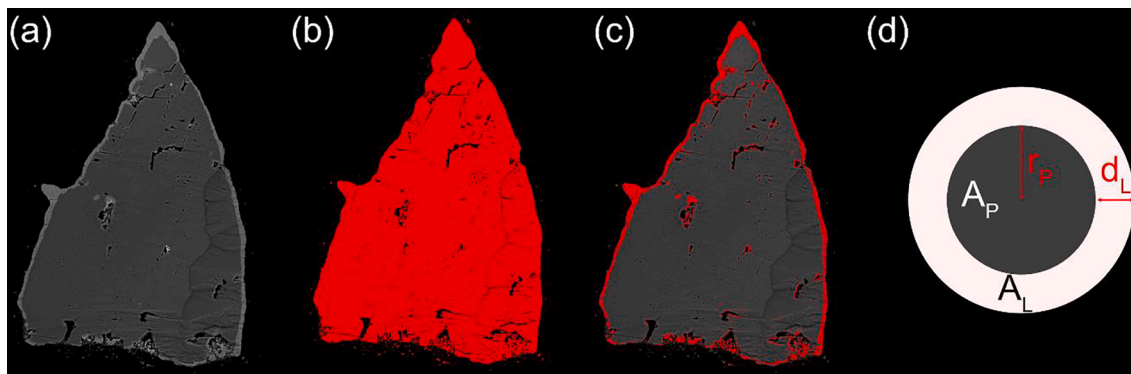

Fig. 2. Illustration of the differentiation between particle and ash layer done with ImageJ: (a) shows the electron micrograph; (b) shows the total area (A_T) of particle and ash layer; (c) shows the area selected as only the ash layer (A_L); (d) provides an overview of the variables used for calculating the ash layer thickness.
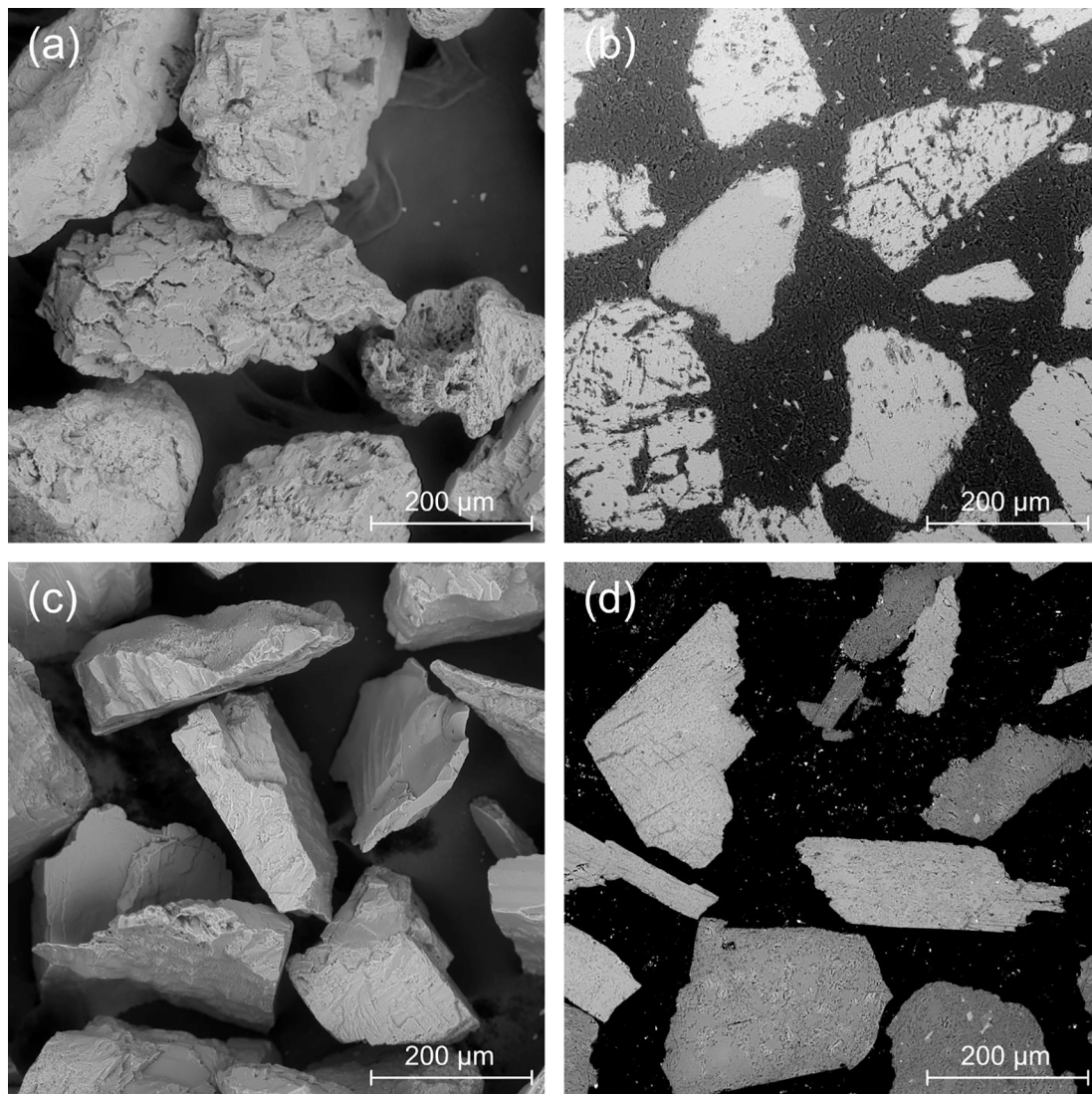
Fig. 3. SEM micrographs showing a top-view (a) and a cross-section (b) of the fresh K-feldspar particles used as bed material in the present study. For comparison, fresh alkali-feldspar analyzed in a different set of experiments conducted in the Chalmers gasifier [20–21] is shown as well: (c) top-view and (d) cross-section.

3.2. BIB cross-sections

Fig. 4 shows higher magnification SEM cross-section micrographs representing the ash accumulation on the particles' edges after 4 and 8 h of exposure to bark, chicken manure and mixtures thereof. Fig. 5 (a) and (b) show the interaction of bark with K-feldspar after 4 and 8 h respectively. The figures show that bark, as a relatively ash-lean fuel (bark: 8.1 wt%, chicken manure: 25.4 wt%), does not lead to major layer formation. Instead, it can be observed that the ash interaction is mainly represented by accumulation of small particles in the cavities of the bed material which were present already in the fresh material (see Fig. 3). Inside the cavities, the back scattered electrons (BSE) contrast is brighter than in the bulk particles, which suggests the presence of compounds rich in heavier elements. From EDS analyses performed on the content inside the cavities, compounds characteristically originating from bark ash, such as Ca and Mg, could be found.

Fig. 5 (c) and (e) depict the results of 4 h interaction with chicken manure ash and K-feldspar. The accumulation of small ash particles can be seen in (c) which occurs to the largest extent in the cavities, similar to what was observed for bark. As chicken manure contains a larger ash fraction than bark, more ash particles are collected within the cavities when chicken manure is used as fuel. The composition of the deposits

was analyzed by EDS and an average over 10 points is shown in Table 4. The most abundant elements are Ca and P, which could be present as a calcium phosphate. Hydroxyapatite $[Ca_5(PO_4)_3OH]$ was previously found after thermal conversion of chicken manure [35–36] and is therefore expected even in the present case. In fact, the Ca/P ratio in Table 4 (1.65) is close to that of hydroxyapatite (1.67). Hydroxyapatite is a very stable compound and therefore only few interactions with the bed material are expected. Thus, only limited amounts of small ash particles should get retained in the bed material, as the ash particles are expected to only bind loosely into the cavities of the feldspar particles.

In Fig. 5 (e), a different result for the bed material-ash interaction can be observed. Areas which are bright in BSE contrast can be found deeper inside the particle. EDS analysis revealed the presence of K and S in these areas, which could indicate K_2SO_4 formation. The presence of K_2SO_4 has been observed in previous studies with chicken manure [9,18,36–38] and in sewage sludge [39]. Similar structures can be observed also for the samples extracted after 8 h. Thus, it can be assumed that K_2SO_4 forms during thermal conversion of chicken manure and accumulates preferentially within cavities and over time, migrates through the cavities deeper into the particles.

The addition of bark to chicken manure appears to inhibit the migration of K_2SO_4 into the particles, as can be seen in Fig. 5 (g) and (h)
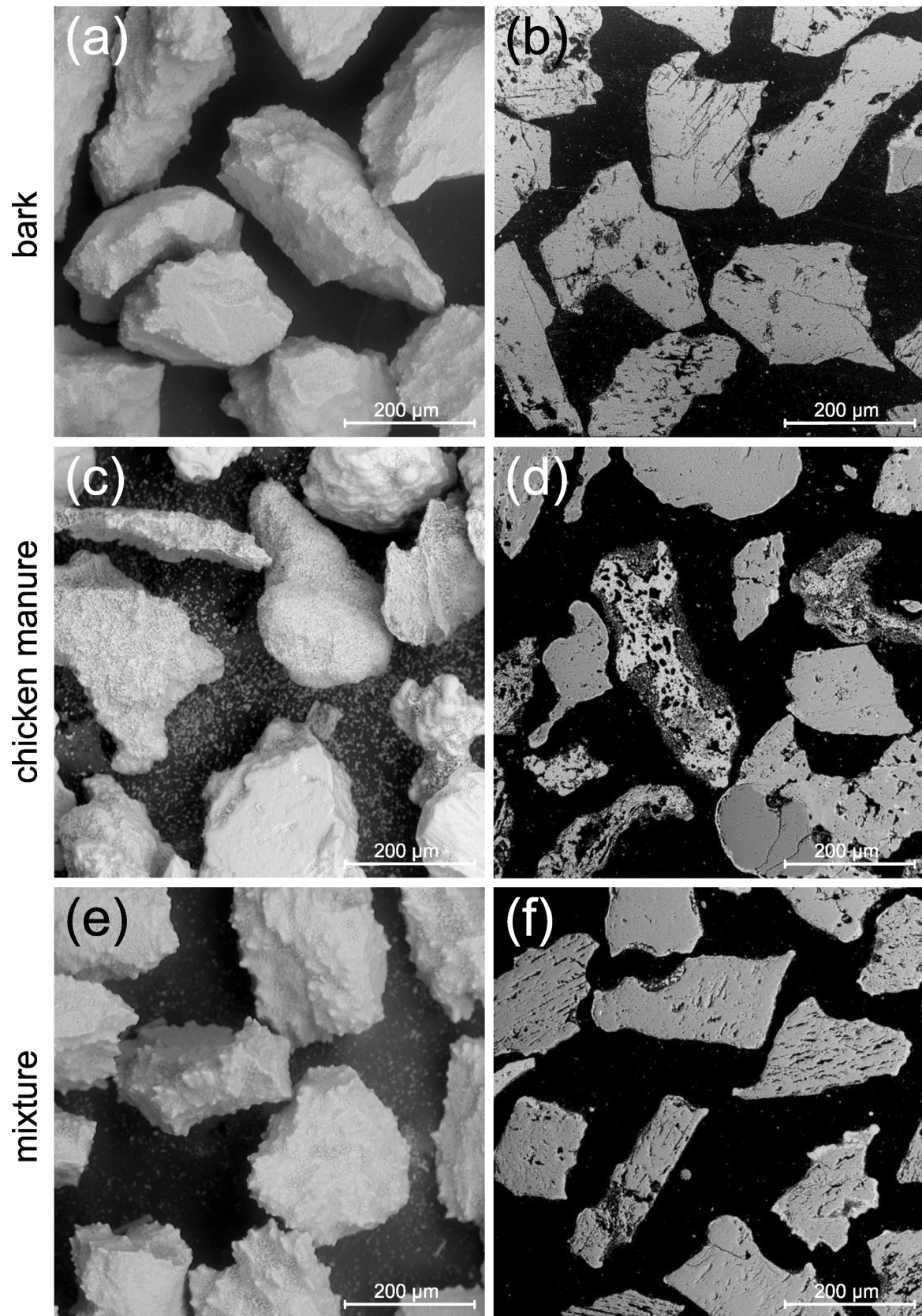
Fig. 4. SEM overviews (left) and SEM cross-sections (right) of the samples taken after 8 h of exposure to fluidized bed conditions, the used fuel being respectively: (a, b) 100 wt% bark, (c, d) 100 wt% chicken manure, (e, f) mixture of 30 wt% chicken manure and 70 wt% bark.
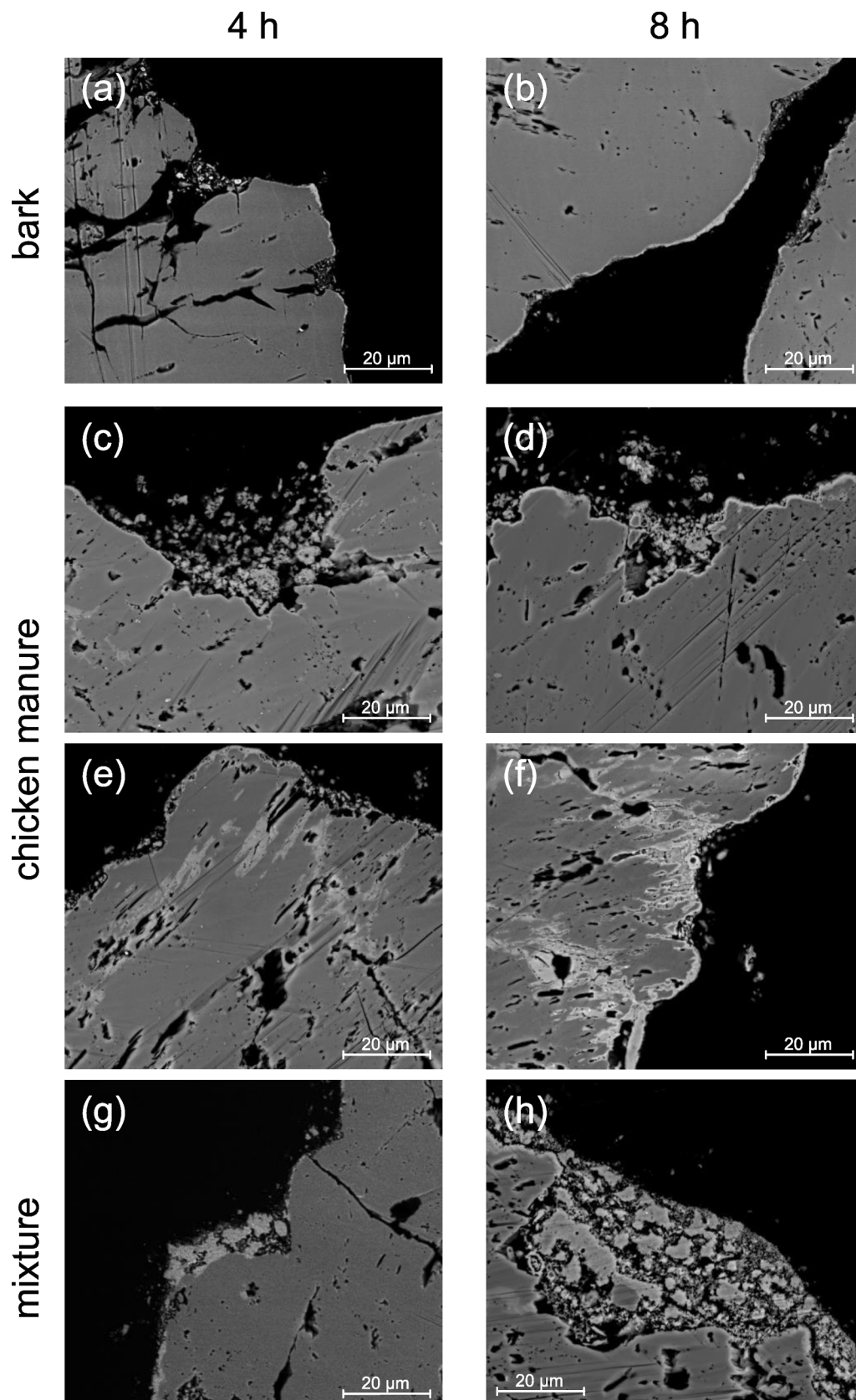
Fig. 5. SEM micrographs of cross-sections produced using BIB of the investigated samples. Left: 4 h samples, bark (a), chicken manure (c and e), mixture of 30 wt% chicken manure and 70 wt% bark (g). Right: 8 h samples, bark (b), chicken manure (d and f), mixture of 30 wt% chicken manure and 70 wt% bark (h).
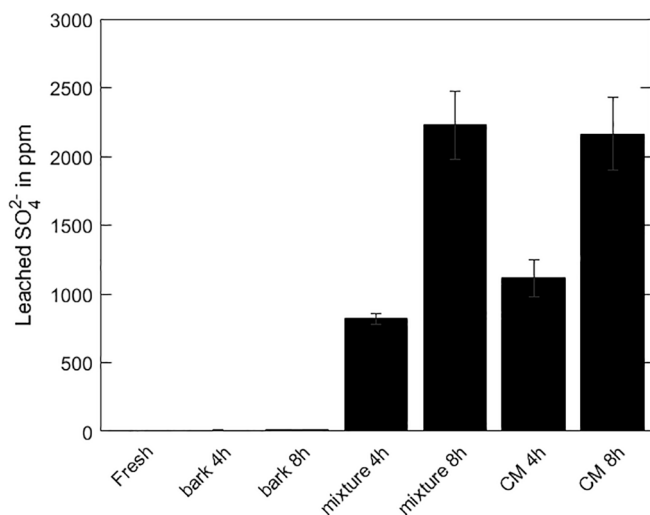
Table 4
Average EDS composition of 10 analysis points recorded on the outer deposits of particles exposed to chicken manure for 4 h (data normalized to an O- and C-free basis and shown in atomic percent).

	Na	Mg	Al	Si	P	S	K	Ca
Concentration [at.%]	0.2	10.1	3.4	12.7	25.9	2.1	3.2	42.4
Standard deviation	0.4	4.1	1.1	2.7	2.3	1.1	0.9	2.9

where the brighter contrast is observed only in surface vicinity. Interestingly, the water-leachable amount of SO_4^{2-} remains constant between the samples exposed to chicken manure and the mixture (see Fig. 6). This is surprising, as the total amount of ash (and therewith the SO_4^{2-} concentration) is higher in the sample where only chicken manure was used as fuel. This suggests that when bark is added to the chicken manure, the phase containing SO_4^{2-} exhibits a higher water solubility or is more accessible to water during the leaching. This could be explained by the formation of thicker layers which was the case of the mixture instead of larger ash particles which were formed in the case of pure chicken manure. Ash compounds located as layers around the particles are expected to be more accessible for leaching than those located in larger ash particles. The formation of thicker layers possibly due to the addition of bark to chicken manure implies the formation of molten phases which could facilitate the retention of small ash particles. The formation of amorphous silicophosphates has previously been reported by Häggström et al. [9], where quartz was used as bed material. In the present study, the Si required for the formation of molten silicophosphates could have been provided by the bark which contains higher amounts of Si compared to chicken manure. Plant-derived Si is mostly present as an amorphous silicate which would facilitate its deposition onto the particles [40].

The speciation of phosphorus plays a major role regarding plant availability [41–43]. The formation of an amorphous phosphorus-containing phase could be interesting for the application of the used bed material as a fertilizer, because amorphous phosphorus showed a higher plant availability than crystalline phosphorus [10,37,44]. Alternatively, the formation of alkali-phosphates was found to increase the fertilization value of phosphorus-rich sewage sludge ash [45–46]. However, both the formation of amorphous phosphorus or alkali-phosphate could be limited if the available P is inherently bound in a stable Ca-phosphate [41]. This was investigated by Hannl et al. [47], where the addition of a K-rich fuel to P-rich sewage sludge was calculated to be beneficial for the formation of K-phosphates. The authors found that the formation of a molten phase could improve the kinetics required for the interaction of the stable Ca-phosphates originating from sewage sludge with K-rich fuel. Subsequent cooling would precipitate K-phosphates which exhibit higher plant availability than Ca-phosphates. In the present study, the formation of a mixed phase containing K, S, Ca, Si and P was found (see Fig. 7 and Fig. 8), when bark was added to chicken manure. The addition of Si from bark leading to the formation of a molten phase could therefore have facilitated the retention of Ca-phosphate particles and the subsequent interaction with K, which agrees with the mechanism described by Hannl et al. [47].

Based on the presented observations, depending on the content of ash and its speciation, the ash either accumulates and forms larger ash particles (as in the case of pure chicken manure) or forms layers on bed material either by adhesion or chemical interaction. This effect is amplified when ash-rich chicken manure is utilized together with bark, possibly because the Si from the bark interacts with the P from chicken manure to form silicophosphates. From the performed observations it can be assumed that the cavities inherently present in the bed material, which was utilized for this study, are the preferred sites for the onset of ash accumulation, including P-enriched compounds. Thus, geometrical artifacts and particle morphology seem to play a significant role for P retention. The feldspar obtained from the sedimentary deposit exhibits lots of cavities which appear to facilitate the deposition of ash particles. Therefore, if the formation of particles with a surface layer rich in P is aimed at, one has to exchange bed more frequently as the material loses its uptake capacity once the cavities are filled. When it comes to chemical affinity of Ca and K, P preferentially is found with Ca in the form of phosphates, whereas K forms predominantly sulphates. Therefore, limiting the presence of Ca through uptake in additives or other forms of removal could enhance the formation of bioavailable K-phosphates.

3.3. Layer analysis

EDS line-scans were recorded on the cross-sections of the samples extracted after 4 h (see Fig. 9). The variations in composition within the ash layers is most likely caused by the heterogeneity of the fuel. The composition acquired from the EDS data was utilized as input data for thermodynamic equilibrium calculations with FactSage 7.2. The conditions for the calculations were set to 830 °C and 1 atm and the elements were assumed to be present in the form of oxides. The results of the calculations are shown in the rightmost column in Fig. 9; for clarity, different Ca- and Mg-silicates [$CaSiO_3$, $CaMg(SiO_3)_2$, Ca_2SiO_4, Mg_2SiO_4, $Ca_2MgSi_2O_7$, and $Ca_3Mg(SiO_4)_2$] were summarized as $(CaO)_x(MgO)_y(SiO_2)_z$.

The figures in the first row shows the results obtained for 100 % bark. The SEM micrograph shows the formation of a thin layer characteristic for a short exposure with relatively ash-lean fuel. The deposition of several small ash particles can also be seen on the micrograph. The EDS line-scan reveals the presence of around 30 % Ca which originates from the fuel ash. At the same time significant amounts of elements present in K-feldspar (~40 % Si, ~10 % Al, and ~ 5 % K) can also be found. This suggests that some of the deposited particles originate from attrition of the bed particles. The FactSage equilibrium calculations suggest the formation of leucite ($KAlSi_2O_6$) and anorthite ($CaAl_2Si_2O_8$) as well as different Ca-Mg-silicates phases. The formation of $KAlSi_2O_6$, and Ca-Mg-silicates is similar to what was found previously when wood was used as fuel and $(K,Na)AlSi_3O_8$ as bed material [20–21].

The result of the interaction of K-feldspar with the mixture of 70 % bark and 30 % chicken manure is shown in the second row of Fig. 9. In the recorded micrograph, a large number of small ash particles can be detected which are collected preferentially in a cavity on the surface of the bed material. Compared to the case with pure bark, the size of the ash particles appears bigger. The EDS line-scan shows around 20–30 at.
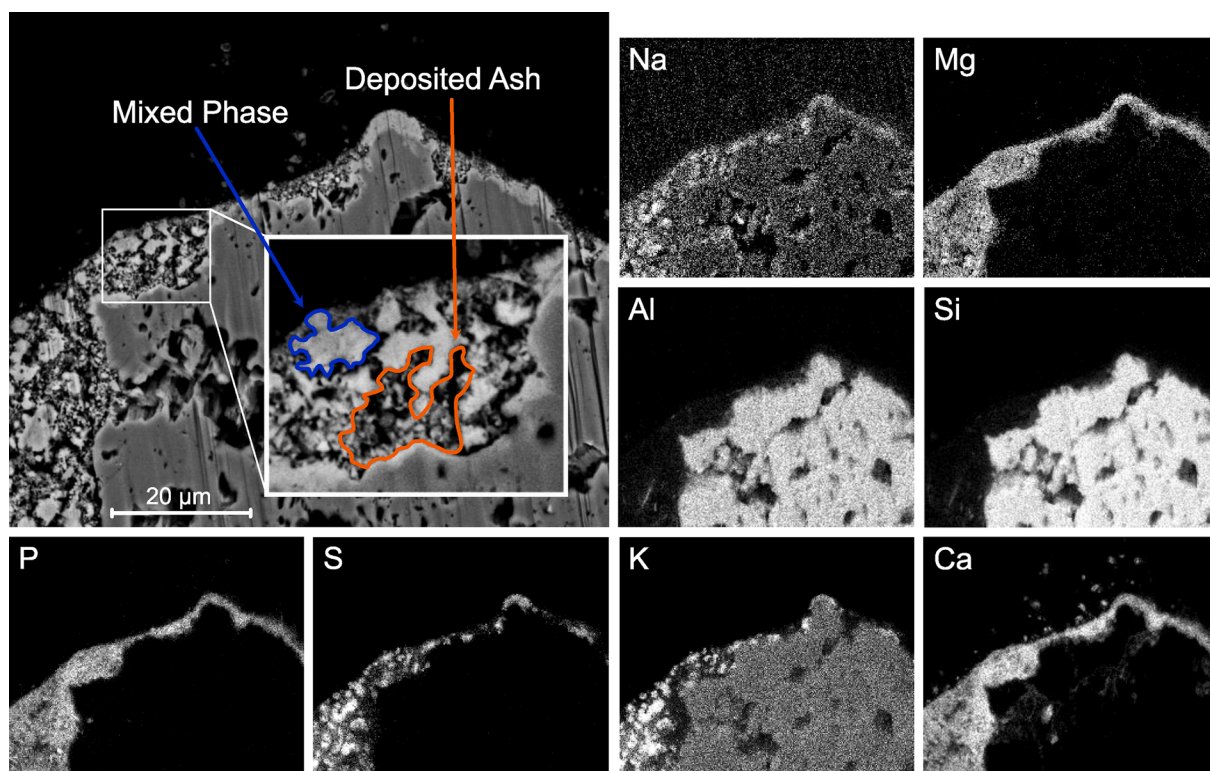

Fig. 6. Ion chromatography results of solubility obtained by leaching trials (L/S (liquid to solid ratio) = 10) of the samples of feldspar exposed to bark, a mixture of bark and chicken manure, and chicken manure (CM) and for 4, respectively 8 h. PO_4^{3-} was not detected by the used instrument which is expected as it is less soluble and therewith less leachable with water.

Fig. 7. BSE micrograph and EDS intensity mapping of the cross-section of a particle exposed to 30 % chicken manure and 70 % bark for 8 h.
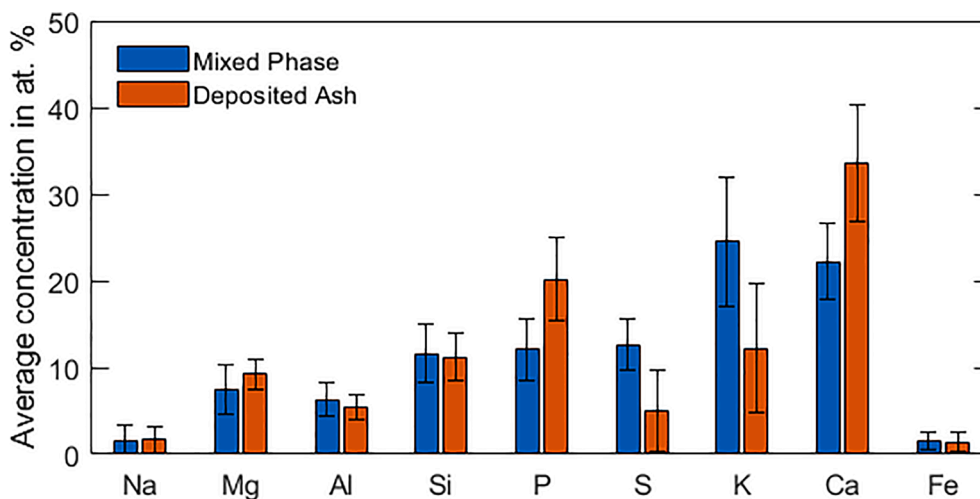

Fig. 8. Average composition of five EDS point analysis recorded on particles exposed to 30 % chicken manure and 70 % bark for 8 h. The error bars indicate the standard deviation between the elemental composition of the EDS points. Points that were aggregated in the 'Mixed Phase' were recorded on the larger particles within the ash layer; 'Deposited Ash' denote the smaller particles in between (see Fig. 7).

% Ca, Si and P on the topmost 2 μm of the layer. The thermodynamic equilibrium calculations based on the EDS results, suggest the formation of $Ca_3(PO_4)_2$ as a stable P-containing phase. Underneath the $Ca_3(PO_4)_2$, the concentration of P decreases, and melt formation is found with FactSage. The formed melt phase could be beneficial for the deposition of ash particles and thereby amplify layer formation. A possible reason for the enhanced retention of ash-derived species could be the deposition of sticky Si which is originally in an amorphous state in biomass [40]. Furthermore, the formation of different sulfates was found on the surface of the particles, consisting of K-sulfate, Ca-sulfate, and a mix thereof. K-sulfate was previously found with X-ray diffraction (XRD) [9,18,48], and was suggested to be beneficial when utilizing the aged

bed material as fertilizer. The addition of Na- or K-sulfate to the combustion of sewage sludge is applied industrially to achieve the formation of Ca(Na,K)PO₄ which is soluble in ammonium citrate and therefore plant-available [45].

The third row on Fig. 9 shows the result of interaction of K-feldspar with pure chicken manure. The previously mentioned deposition of small ash particles can be seen once more. Similar to the case with the mix of bark and chicken manure, a thin continuous layer can be detected on the feldspar particle. The composition of the deposited particles resembles the one detected for the mix, however, when pure chicken manure is applied, the concentration of S in these particles is lower. This is unexpected, as the concentration of S is higher in the ash of pure
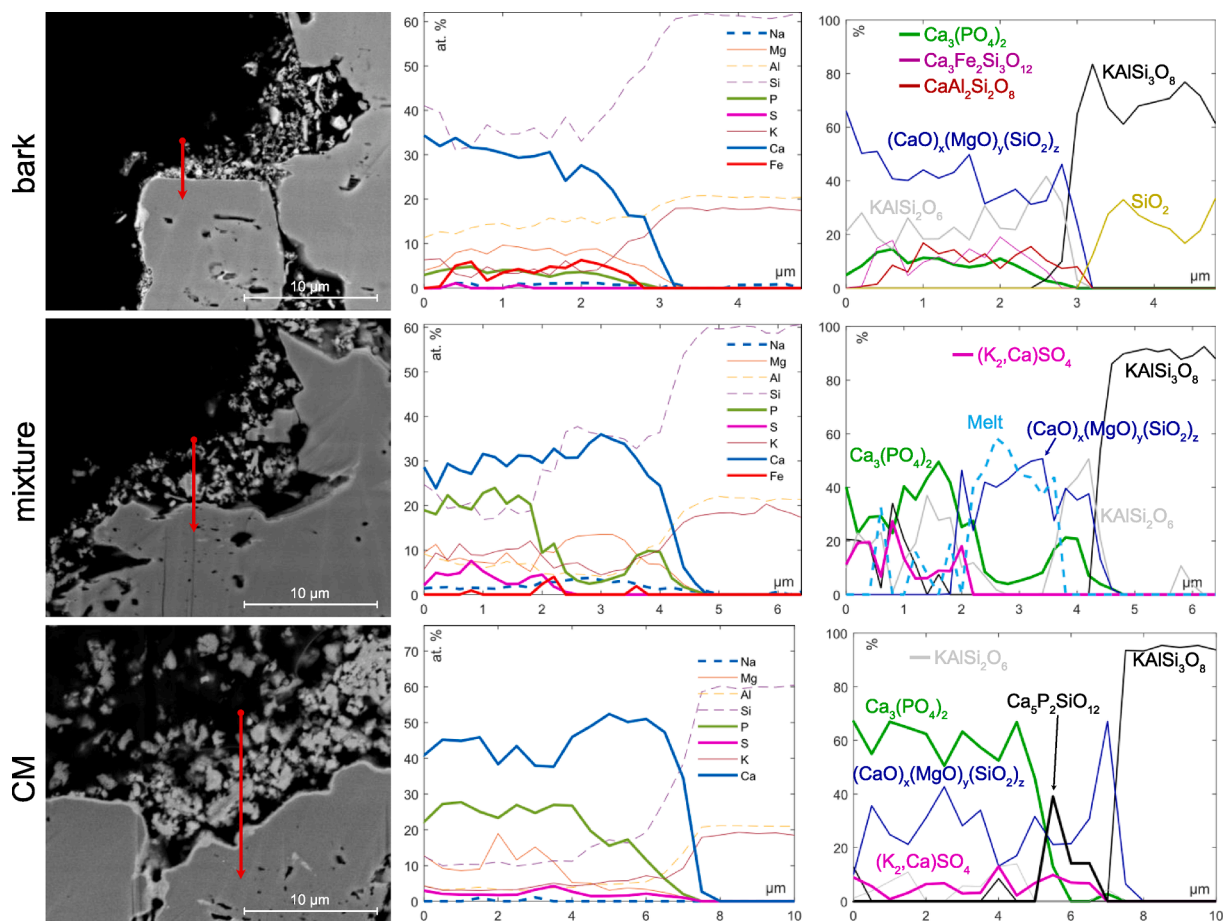
Fig. 9. BSE micrograph (left), EDS line-scan (middle) and thermodynamic equilibrium calculation results (right) of K-feldspar exposed to different conditions for 4 h: First row – 100% bark; second row − 70% bark and 30% chicken manure; third row – 100% chicken manure.

chicken manure and a possible explanation for this could be the migration of K_2SO_4 deeper into cavities present in the particles. Furthermore, the measured compositions do not result in melt formation. This could hinder the deposition of ash particles and therefore be the reason for a comparably thinner average layer formation [15]. At the interface of the deposited ash particles and the bed particle, $Ca_5P_2SiO_{12}$ was calculated to form, which agrees with the previously suggested formation of silicophosphates occurring when different P-rich fuels were thermally converted [9,49–50].

The formation of a surface layer rich in ash elements after only 4 h of interaction time could be beneficial for the application for biomass gasification, where the presence of an ash-layer is required to decrease the concentration of tars in the product gas [16,18].

3.4. Thickness analysis

To quantify the thickness of the ash layers formed around the bed particles, the ImageJ [32] software was used to differentiate between particles and layer. This was done for four particles of the samples obtained after 8 h exposure to chicken manure and the mixture of chicken manure and bark (shown in Fig. 10).

The results of the calculations are shown in Table 5. While the thickness of the ash layers formed around the particles exposed to the mixture were found to be around 30 % thicker, the variation is within the standard deviation. Furthermore, several assumptions had to be made (spherical particles, constant layer thickness), to calculate the thickness of the layer and only four particles were investigated for each sample. However, despite these limitations, the results can confirm the amplification of layer formation when the mixture of bark and chicken

manure is utilized, because the total ash that was added to the reactors differs significantly between the two cases. After 8 h exposure to pure chicken manure, around 1.4 kg ash were added, whereas the amount of ash added from the mixture is about 0.76 kg. Thus, relative to the ash added to the system, the ash layer formation on the particles exposed to the mixture is about twice as thick compared to pure chicken manure. To achieve fast layer formation co-combustion of the two fuels appears to be beneficial.

3.5. Fixed bed salt exposures

To investigate the interaction of K-feldspar and phosphate salts of different alkali and alkaline earth metals (AAEM) in a more controlled environment, fixed bed exposures were conducted for 24 h at 830 °C. The two alkaline earth salts utilized for the exposure were $CaHPO_4$ and $Mg_3(PO_4)_2 \cdot 5H_2O$. Neither of the two salts showed any interaction with K-feldspar, which is why no micrographs are shown here. This agrees with the reported high chemical stability of Ca-phosphates [such as hydroxyapatite ($Ca_5(PO_4)_3OH$)] which tend to form when fuels rich in Ca and P are thermally converted [35–36,44,47–48]. As apatites do not exhibit strong plant-availability, their formation should be avoided if utilization of the spend material as fertilizer is the aim [9,35,41]. The results of the interaction of K-feldspar with K_3PO_4 and $Na_3PO_4 \cdot 12H_2O$ are shown in Fig. 11 (a) and (b) respectively.

Although feldspar is generally considered resistant to agglomeration, agglomeration of the K-feldspar particles was observed in the performed experiments with K_3PO_4. The particles are agglomerated by a phase of brighter BSE contrast which is also present in the cavities found in the fresh bed material. The elemental composition of this phase has a ratio
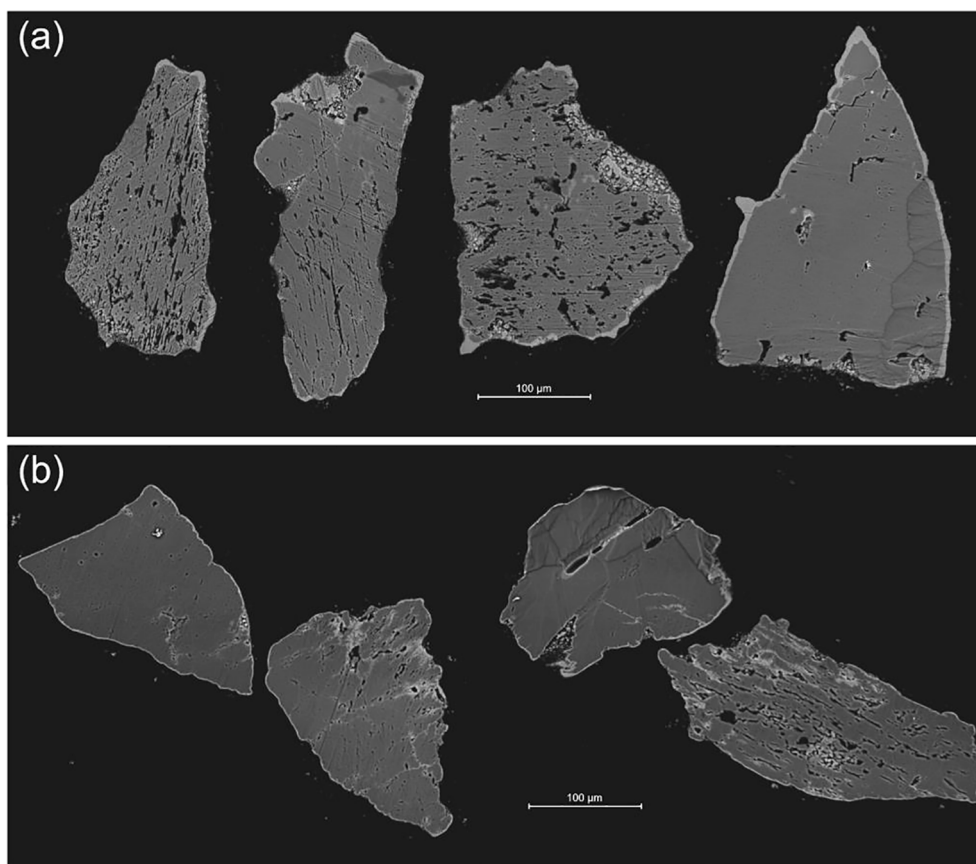
Fig. 10. Back-scattered electron micrographs of bed particles used for layer thickness calculations: (a) bed particles exposed to 70% bark and 30% chicken manure for 8 h; (b) bed particles exposed to 100% chicken manure for 8 h.

Table 5
Results of the ash layer thickness calculations on the samples extracted after 8 h exposure to the mixture of bark and chicken manure, and the samples exposed to pure chicken manure.

	Mixture (70 % bark, 30 % CM)	100 % chicken manure
Average Layer Thickness [μm]	5.5	4.2
Standard Deviation [μm]	1.4	0.7

of K to P of about 2.5, which is close to the original K_3PO_4. This indicates that the agglomeration mechanism is melt induced as only minor interactions occurred between salt and bed material [51]. As feldspar minerals are more prone to weathering than quartz, they exhibit more pores and cavities which could have been points of interaction with the concentrated K_3PO_4. A quartz particle can be found in the bottom left corner of the micrograph which exhibits only limited interaction with K_3PO_4, as the layer around the particle is rather thin. The limited interaction of SiO_2 with K_3PO_4 is in agreement with the ash transformation chemistry described by Boström et al. [52], where K preferably interacts with phosphate rather than silicate. In the case of Na_3PO_4, weaker interaction with K-feldspar is seen. Agglomeration can still be observed; however, the formed agglomerates are smaller in size than with K_3PO_4. According to publications on the plant-availability of phosphorus-rich ash, the formation of an amorphous phosphorus phase was found to be preferred (most available) [10,13,44]. The present results indicate that during the addition of K or Na to support the formation of an amorphous phosphate, agglomeration could be an issue.

4. Mechanism

The suggested interactions occurring for the three different cases of fuel and K-feldspar, used as a bed material that were investigated for this study, are schematically shown in Fig. 12. In the case of pure bark used as fuel (depicted on the left), Ca and Si present in bark ash led to the formation of a thin Ca-silicate layer, which can retain smaller particles caused by attrition of the feldspar particles. When chicken manure is added to the bark as a fuel (depicted on the top), the alkali-sulfates from the ash can interact with the Ca-silicate and amplify the layer formation. This layer is likely to be in a molten state which enables retention of Ca-phosphate particles from the ash. The Ca-phosphates are preferentially collected in the cavities present in the bed particles, where their retention enables interaction with the molten layer underneath. This interaction can cause diffusion of P into the molten layer. If solely chicken manure is utilized as fuel (depicted on the right), no Ca-silicate layer forms, which hampers the retention of P-rich ash particles and the ash-derived alkali-sulfate migrates deeper into the feldspar, where it fills pores and cavities. Due to the high amount of ash in the reactor, larger ash particles are formed consisting of phosphates and sulfates.

Hence, the mechanism of early layer formation on the bed particles has a strong dependence on the fuel ash composition and the morphology of the bed material. The utilization of a bed material with a high number of cavities appears to facilitate retention of deposited ash. The short interaction time of the particles investigated in the current study led to the formation of layers consisting mostly of ash-derived elements and was insufficient for the formation of inner interaction layers. This agrees with the review on layer formation on bed material by Kuba et al. [25]. Feldspar was described to exhibit a weaker tendency to form an inner interaction layer compared to olivine and quartz [25]. Exposure of feldspar to P-rich fuel was found to only form outer layers on
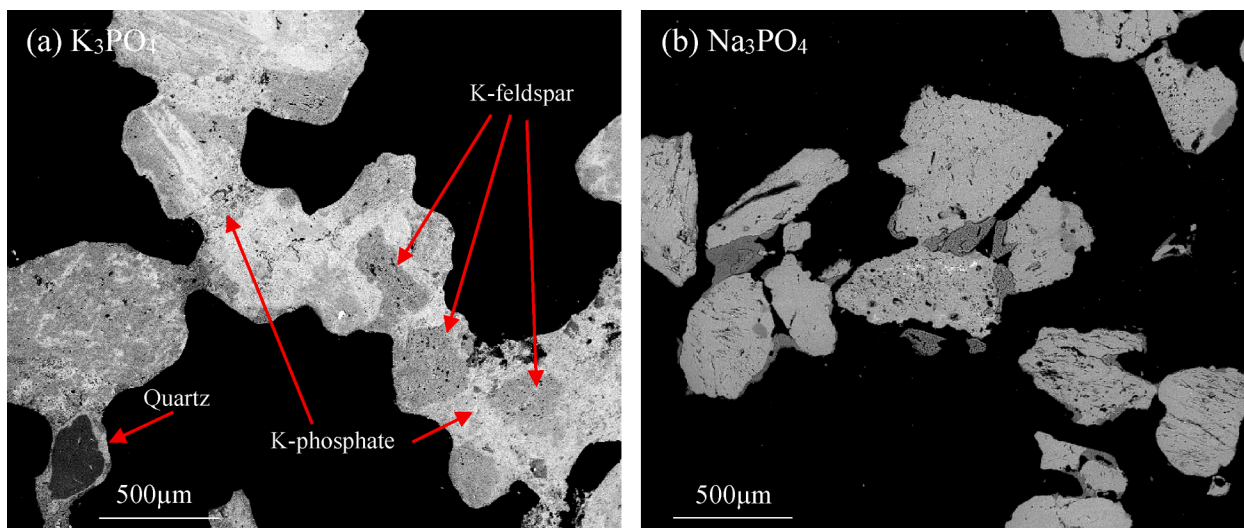
Fig. 11. SEM micrographs of the cross-section of K-feldspar exposed to K3PO4 (a) and Na3PO4 (b) in fixed bed laboratory conditions at 830 °C for 24 h.
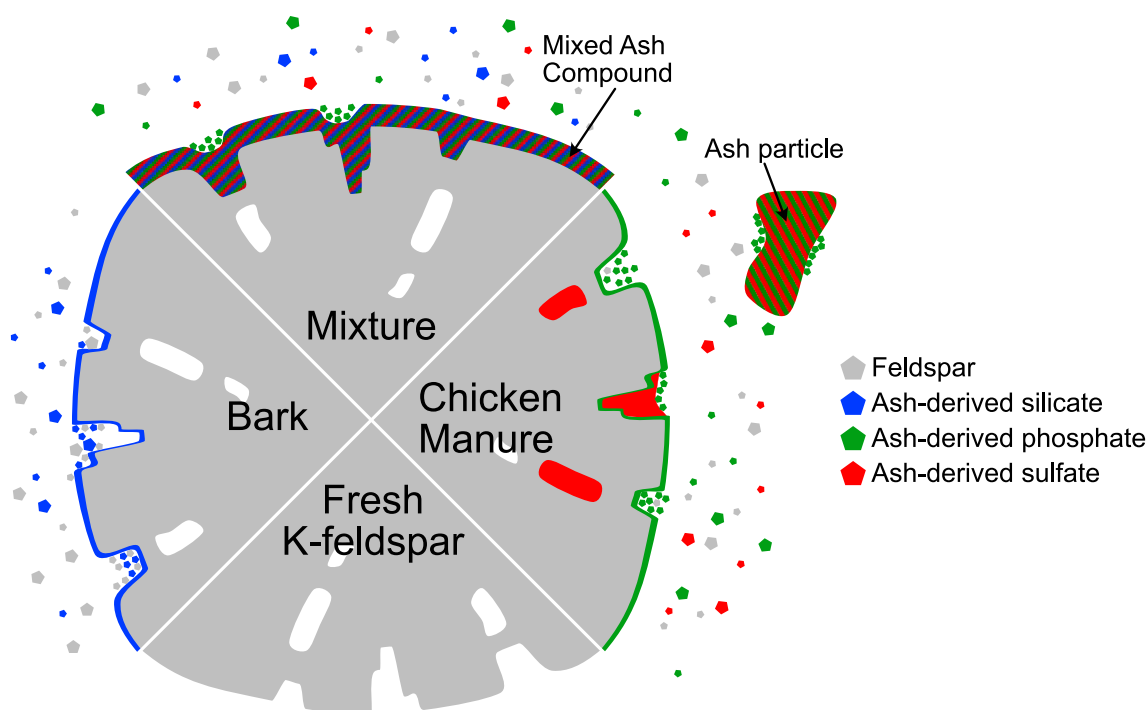

Fig. 12. Illustration of suggested mechanism of bed material/fuel ash interaction for the three different fuel cases (bark, bark/chicken manure, chicken manure).

bed particles [25], which was confirmed in the present study. This was explained by the reaction of P with fuel ash elements instead of the bed particles. In the present study, the interaction between ash of different fuels is elucidated and new insights were obtained regarding the influence of the morphology of the fresh material.

5. Conclusion

Based on the described results, the deposition and accumulation of fuel ash is dependent on the presence of uneven surfaces such as cavities within the particles. The presence of these cavities allows the enclosure of P in the form of calcium phosphate from the chicken manure ash. Depending on the ash composition, the calcium phosphate stays unchanged or can further interact with the bed material. The addition of bark enhances the formation of an ash layer and therefore the retention

of P on the particles. A possible reason for this could be the amorphous state of biomass ash-derived Si. The enhanced layer formation when the mixture of bark and chicken manure is utilized, can positively affect the development of catalytic activity of the particles. Furthermore, interaction of Ca-phosphate (originating from chicken manure ash) with K is required to obtain a more bioavailable amorphous K- and P-rich phase. This exchange is promoted as well by the co-combustion of bark and chicken manure. However, further research is required to investigate the bioavailability of the phosphates formed in the different cases.

Based on the obtained results, if the goal is to accumulate P on the surface of the bed material, the co-combustion of chicken manure with a K- and Si-rich fuel is likely to be beneficial and the bed material should exhibit cavities which facilitate the deposition of ash particles. As the deposition of ash alters the morphology of the bed material, frequent replacement of the bed inventory is likely to augment P-retention.

The results obtained in this study are based on SEM employing a time-intensive sample preparation method. Therefore, only a limited number of particles can be analyzed which decreases the representativity of the results. However, the conclusions drawn in this study agree with the results obtained by previous research on the same samples. Thus, the details added by the methods utilized in this study provide valuable insight into the impact of bed particle morphology and the interaction of the ash fractions from bark and chicken manure.

CRediT authorship contribution statement

Robin Faust: Methodology, Investigation, Writing – original draft, Writing – review & editing. **Katharina Fürsatz:** Resources, Writing – original draft, Writing – review & editing. **Panida Aonsamang:** Investigation. **Marcus Sandberg:** Investigation. **Matthias Kuba:** Writing – review & editing, Supervision, Funding acquisition. **Nils Skoglund:** Writing – review & editing, Supervision, Funding acquisition. **Pavleta Knutsson:** Conceptualization, Writing – review & editing, Supervision, Funding acquisition.

Declaration of Competing Interest

The authors declare that they have no known competing financial interests or personal relationships that could have appeared to influence the work reported in this paper.

Data availability

Data will be made available on request.

Acknowledgements

References

[1] IPCC, 2019: Climate Change and Land: an IPCC special report on climate change, desertification, land degradation, sustainable land management, food security, and greenhouse gas fluxes in terrestrial ecosystems [P.R. Shukla, J. Skea, E. Calvo Buendia, V. Masson-Delmotte, H.-O. Pörtner, D. C. Roberts, P. Zhai, R. Slade, S. Connors, R. van Diemen, M. Ferrat, E. Haughey, S. Luz, S. Neogi, M. Pathak, J. Petzold, J. Portugal Pereira, P. Vyas, E. Huntley, K. Kissick, M. Belkacemi, J. Malley, (eds.)]. In press.
[2] Steffen W, Richardson K, Rockström J, Cornell SE, Fetzer I, Bennett EM, et al. Planetary boundaries: Guiding human development on a changing planet. Science 2015;347(6223).
[3] U.N. General Assembly Transforming our world : the 2030 Agenda for Sustainable Development, 21, A/RES/70/1 https://www.refworld.org/docid/57b6e3e44.html October 2015 available at: accessed 9 December 2021.
[4] Conley DJ, Paerl HW, Howarth RW, Boesch DF, Seitzinger SP, Havens KE, et al. Controlling Eutrophication: Nitrogen and Phosphorus. Science 2009;323(5917): 1014–5.
[5] Chang H, Yoo D, Lim H, Ahn K, Park N, Jang Y, et al. Granular crystallization using CFBC ash for phosphorus removal via hydroxyapatite. Environ Technol Innov 2021;21:101173.
[6] Baranzelli C, Blagoeva D, Blengini GA, Ciupagea C, Dewulf J, Dias P, et al. Methodology for establishing the EU list of critical raw materials: guidelines. 2017 [cited 2021 Jul 9]; Available from: http://dx.publications.europa.eu/10.2873/769526.
[7] Link S, Yrjas P, Lindberg D, Trikkel A, Mikli V. Ash melting behaviour of reed and woody fuels blends. Fuel 2022;314:123051.
[8] Espindola J, Selim OM, Amano RS. Co-Pyrolysis of Rice Husk and Chicken Manure. J Energy Resour Technol 2021 Feb 1;143(2):022101.
[9] Häggström G, Fürsatz K, Kuba M, Skoglund N, Öhman M. Fate of Phosphorus in Fluidized Bed Cocombustion of Chicken Litter with Wheat Straw and Bark Residues. Energy Fuels 2020 Feb 20;34(2):1822–9.
[10] Więckol-Ryk A, Białecka B, Cempa M, Adamczyk Z. Optimization of chicken manure combustion parameters in the aspect of phosphorus recovery. Int J Recycl Org Waste Agric 2020 Jul;9:273–85.
[11] Delin S. Fertilizer value of phosphorus in different residues. Soil Use Manag 2016 Mar;32(1):17–26.
[12] Williams AG, Leinonen I, Kyriazakis I. Environmental benefits of using turkey litter as a fuel instead of a fertiliser. J Clean Prod 2016 Feb;113:167–75.
[13] Hosho F. Phosphorus Recovery from Sewage Sludge by High-Temperature Thermochemical Process (KUBOTA Process). In: Ohtake H, Tsuneda S, editors. Phosphorus Recovery and Recycling [Internet]. Singapore: Springer Singapore; 2019. p. 189–99. Available from: https://doi.org/10.1007/978-981-10-8031-9_12.
[14] Hagman H, Backman R, Boström D. Effects on a 50 MW th Circulating Fluidized-Bed Boiler Co-firing Animal Waste, Sludge, Residue Wood, Peat, and Forest Fuels. Energy Fuels 2013 Oct 17;27(10):6146–58.
[15] Wagner K, Häggström G, Skoglund N, Priscak J, Kuba M, Öhman M, et al. Layer formation mechanism of K-feldspar in bubbling fluidized bed combustion of phosphorus-lean and phosphorus-rich residual biomass. Appl Energy 2019;248: 545–54.
[16] Berguerand N, Marinkovic J, Berdugo Vilches T, Thunman H. Use of alkali-feldspar as bed material for upgrading a biomass-derived producer gas from a gasifier. Chem Eng J 2016 Jul;295:80–91.
[17] Berguerand N, Berdugo VT. Alkali-Feldspar as a Catalyst for Biomass Gasification in a 2-MW Indirect Gasifier. Energy Fuels 2017 Feb 16;31(2):1583–92.
[18] Fürsatz K, Kuba M, Janisch D, Aziaba K, Hammerl C, Chlebda D, et al. Impact of residual fuel ash layers on the catalytic activation of K-feldspar regarding the water–gas shift reaction. Biomass Convers Biorefinery 2021;11(1):3–14.
[19] Pissot S. Strategies for Complete Recovery of Carbon in Dual Fluidized Bed Gasifiers [PhD Thesis]. [Gothenburg]: Chalmers Univerity; 2021.
[20] Hannl TK, Faust R, Kuba M, Knutsson P, Berdugo Vilches T, Seemann M, et al. Layer Formation on Feldspar Bed Particles during Indirect Gasification of Wood. 2. Na-Feldspar. Energy Fuels 2019;33(8):7333–46.
[21] Faust R, Hannl TK, Vilches TB, Kuba M, Öhman M, Seemann M, et al. Layer Formation on Feldspar Bed Particles during Indirect Gasification of Wood. 1. K-Feldspar. Energy Fuels 2019;33(8):7321–32.
[22] Morris JD, Daood SS, Chilton S, Nimmo W. Mechanisms and mitigation of agglomeration during fluidized bed combustion of biomass: A review. Fuel 2018 Oct;230:452–73.
[23] Nascimento FRM, González AM, Silva Lora EE, Ratner A, Escobar Palacio JC, Reinaldo R. Bench-scale bubbling fluidized bed systems around the world - Bed agglomeration and collapse: A comprehensive review. Int J Hydrog Energy 2021 May;46(36):18740–66.
[24] Fürsatz K, Fuchs J, Benedikt F, Kuba M, Hofbauer H. Effect of biomass fuel ash and bed material on the product gas composition in DFB steam gasification. Energy 2021;219:119650.
[25] Kuba M, Skoglund N, Öhman M, Hofbauer H. A review on bed material particle layer formation and its positive influence on the performance of thermo-chemical biomass conversion in fluidized beds. Fuel 2021;291:120214.
[26] Wagner K, Häggström G, Mauerhofer AM, Kuba M, Skoglund N, Öhman M, et al. Layer formation on K-feldspar in fluidized bed combustion and gasification of bark and chicken manure. Biomass Bioenergy 2019;127:105251.
[27] Kuba M, He H, Kirnbauer F, Skoglund N, Boström D, Öhman M, et al. Thermal Stability of Bed Particle Layers on Naturally Occurring Minerals from Dual Fluid Bed Gasification of Woody Biomass. Energy Fuels 2016;30(10):8277–85.
[28] Grimm A, Skoglund N, Boström D, Öhman M. Bed Agglomeration Characteristics in Fluidized Quartz Bed Combustion of Phosphorus-Rich Biomass Fuels. Energy Fuels 2011 Mar 17;25(3):937–47.
[29] Öhman M, Nordin A. A New Method for Quantification of Fluidized Bed Agglomeration Tendencies: A Sensitivity Analysis. Energy Fuels 1998 Jan 1;12(1): 90–4.
[30] Faust R, Berdugo Vilches T, Malmberg P, Seemann M, Knutsson P. Comparison of Ash Layer Formation Mechanisms on Si-Containing Bed Material during Dual Fluidized Bed Gasification of Woody Biomass. Energy Fuels 2020 Jul 16;34(7): 8340–52.
[31] Faust R, Sattari M, Maric J, Seemann M, Knutsson P. Microscopic investigation of layer growth during olivine bed material aging during indirect gasification of biomass. Fuel 2020;266:117076.
[32] Schneider CA, Rasband WS, Eliceiri KW. NIH Image to ImageJ: 25 years of image analysis. Nat Methods 2012 Jul;9(7):671–5.
[33] Bale CW, Bélisle E, Chartrand P, Decterov SA, Eriksson G, Gheribi AE, et al. FactSage thermochemical software and databases, 2010–2016. Calphad 2016;54: 35–53.
[34] Tafler D, Colomer E. POTASSIUM FELDSPARS WITH LOW IRON AND SODIUM CONTENTS FOR CERAMIC FRIT AND GLAZE PRODUCTION. In: Qualicer 96 IV World Congress on Ceramic Tile Quality General Conferences and Proceedings. Castellon; 1996. (13; vol. 10).
[35] Pandey DS, Yazhenskikh E, Müller M, Ziegner M, Trubetskaya A, Leahy JJ, et al. Transformation of inorganic matter in poultry litter during fluidised bed gasification. Fuel Process Technol 2021;221:106918.
[36] Lynch D, Henihan AM, Kwapinski W, Zhang L, Leahy JJ. Ash Agglomeration and Deposition during Combustion of Poultry Litter in a Bubbling Fluidized-Bed Combustor. Energy Fuels 2013 Aug 15;27(8):4684–94.
[37] Adamczyk Z, Cempa M, Białecka B. Phosphorus-Rich Ash from Poultry Manure Combustion in a Fluidized Bed Reactor. Minerals 2021 Jul 20;11(7):785.
[38] Nuutinen LH, Tiainen MS, Virtanen ME, Enestam SH, Laitinen RS. Coating Layers on Bed Particles during Biomass Fuel Combustion in Fluidized-Bed Boilers. Energy Fuels 2004 Jan 1;18(1):127–39.
[39] Skoglund N, Grimm A, Öhman M, Boström D. Combustion of Biosolids in a Bubbling Fluidized Bed, Part 1: Main Ash-Forming Elements and Ash Distribution with a Focus on Phosphorus. Energy Fuels 2014 Feb 20;28(2):1183–90.

[40] Conley DJ. Terrestrial ecosystems and the global biogeochemical silica cycle: GLOBAL BIOGEOCHEMICAL SILICA CYCLE. Glob Biogeochem Cycles 2002;16(4): 68-1.

[41] Falk J, Skoglund N, Grimm A, Öhman M. Fate of Phosphorus in Fixed Bed Combustion of Biomass and Sewage Sludge. Energy Fuels 2020 Apr 16;34(4): 4587–94.

[42] Imai T. Calcination Technology for Manufacturing Mineral Fertilizer Using CaO-Enriched Sewage Sludge Ash. In: Ohtake H, Tsuneda S, editors. Phosphorus Recovery and Recycling [Internet]. Singapore: Springer; 2019 [cited 2021 Jul 8]. p. 179–87. Available from: https://doi.org/10.1007/978-981-10-8031-9_11.

[43] Eurostat. Nutrient Budgets - Methodology and Handbook. Version 1.02. Luxemburg: Eurostat and OECD; 2013.

[44] Nanzer S, Oberson A, Huthwelker T, Eggenberger U, Frossard E. The Molecular Environment of Phosphorus in Sewage Sludge Ash: Implications for Bioavailability. J Environ Qual 2014 May;43(3):1050–60.

[45] Sludge Ash. In: Ohtake H, Tsuneda S, editors. Phosphorus Recovery and Recycling [Internet]. Singapore: Springer Singapore; 2019. p. 221–33. Available from: https://doi.org/10.1007/978-981-10-8031-9_15.

[46] Herzel H, Krüger O, Hermann L, Adam C. Sewage sludge ash — A promising secondary phosphorus source for fertilizer production. Sci Total Environ 2016 Jan; 542:1136–43.

[47] Hannl TK, Sefidari H, Kuba M, Skoglund N, Öhman M. Thermochemical equilibrium study of ash transformation during combustion and gasification of sewage sludge mixtures with agricultural residues with focus on the phosphorus speciation. Biomass Convers Biorefinery 2021 Feb;11(1):57–68.

[48] Rivera R, Chagnes A, Cathelineau M, Boiron MC. Conditioning of poultry manure ash for subsequent phosphorous separation and assessment for a process design. Sustain Mater Technol. 2022 Apr;31:e00377.

[49] Li F, Li Y, Zhao C, Fan H, Xu M, Guo Q, et al. Investigation on Ash-Fusion Characteristics of Livestock Manure and Low-Rank Coals. Energy Fuels 2020;34(5): 5804–12.

[50] Häggström G, Hannl TK, Hedayati A, Kuba M, Skoglund N, Öhman M. Single Pellet Combustion of Sewage Sludge and Agricultural Residues with a Focus on Phosphorus. Energy Fuels 2021 Jun 17;35(12):10009–22.

[51] Brus E, Öhman M, Nordin A. Mechanisms of Bed Agglomeration during Fluidized-Bed Combustion of Biomass Fuels. Energy Fuels 2005 May;19(3):825–32.

[52] Boström D, Skoglund N, Grimm A, Boman C, Öhman M, Broström M, et al. Ash Transformation Chemistry during Combustion of Biomass. Energy Fuels 2012;26 (1):85–93.